Numerical Modeling of Lateral Response of Long Flexible Piles in Sand

Md. Iftekharuzzaman[1] and Bipul C Hawlader[2]*
[1]*Faculty of Engineering and Applied Science, Memorial University, St. John's, NL A1B 3X5, Canada*
[2]*Faculty of Engineering and Applied Science, Memorial University, St. John's, NL A1B 3X5*
**E-mail*: bipul@mun.ca

ABSTRACT: The behavior of a steel pipe pile in sand subjected to lateral load is examined by finite element (FE) analysis. Three-dimensional finite element analyses are performed for pure lateral load applied at 0.3m above the ground surface. The FE analyses are performed using the commercially available software package ABAQUS/Standard. The sand around the pile is modeled using a modified form of Mohr-Coulomb soil constitutive model. The modification involves the variation of mobilized angle of internal friction and dilation angle with plastic shear strain. The nonlinear variation of elastic modulus with mean effective stress is also considered in the present FE analyses. These important features of soil constitutive model have been implemented in ABAQUS/Standard using a user subroutine. Numerical analyses are also performed by using the LPILE software, which is based on the *p-y* curve. The FE and LPILE results are compared with the results of a full-scale test. It is shown that the FE analysis with modified Mohr-Coulomb soil model can successfully simulate better the response of a pile under lateral load. Comparing the numerical results with the full-scale test results some limitations of the *p-y* curve method are highlighted.

1. INTRODUCTION

The lateral resistance of pile foundations is one of the key design considerations in many civil engineering structures both in onshore and offshore environment. Wind, wave, earthquake and ground movement might create significant lateral load on pile foundations. If the deformation and bending moment induced by lateral load are confined only to the upper part the pile is considered as flexible pile. The response of a pile under lateral load is governed by complex three-dimensional soil/pile interaction behaviour. Various approaches have been proposed in the past for analysis of a laterally loaded pile. As the main focus of the present study is to investigate the response of a free-headed single steel pipe pile in sand under lateral load, a review of previous studies related to this area are presented in the following sections.

Hansen (1961) proposed a method for estimating the ultimate lateral load resistance of vertical piles based on earth pressure theory. Broms (1964 a, b) also proposed methods for calculating the ultimate lateral resistance based on earth pressure theory simplifying the analyses for cohesionless and cohesive soils for short rigid and long flexible piles. Meyerhof et al. (1981, 1988) also proposed methods to estimate the ultimate lateral resistance and groundline displacement at the working load for rigid and flexible piles.

The lateral deflection of pile head is one of the main requirements in the current design practice, especially in limit state design. Mainly two approaches are currently used for modeling the lateral load deflection behaviour of piles. In the first approach, the response of soil under lateral load is modeled using nonlinear independent springs in the form of *p-y* curves, where *p* is the soil-pile reaction (i.e. the force per unit length of the pile) and *y* is the lateral deflection of the pile. Then using the concept of beam-on-elastic foundation the problem is solved numerically. The *p-y* curve method is very similar to the subgrade reaction method except that in the *p-y* curve method the soil resistance is nonlinear while in the subgrade reaction method it is linear with displacement. Reese et al. (1974) proposed a method to define the *p-y* curves for static and cyclic loading. A modified version of Reese et al. (1974) is employed by the American Petroleum Institute (API 2000) in its manual for recommended practice. Both of these models have been implemented in the commercially available software LPILE Plus 5.0 (2005). Ashour and Norris (2000) showed that the "Strain Wedge" model is capable of evaluating some additional effects such as bending stiffness of the pile, pile shape, pile head fixity and depth of embedment on the *p-y* curves. The second approach of modeling laterally loaded piles is based on continuum modeling. Poulos (1971) presented finite element analysis of a single pile situated in an ideal elastic soil mass. Finite element analyses of single piles under lateral load have also been conducted by other researchers (Brown and Shie 1991, Kimura et al. 1995, Wakai et al. 1999, Yang and Jeremic 2002). Brown and Shie (1991) performed three-dimensional finite element analysis modeling the soil using von Mises and extended Drucker-Prager constitutive model. Trochanis et al. (1991) examined the effects of nonlinearity in soil stress-strain behaviour and separation or slippage between the soil and the pile surfaces. In addition, there are some full-scale test results (e.g. Cox et al. 1974, Long and Reese 1985, Brown 1985, Rollins et al. 2005, Ruesta and Townsend 1997) and centrifuge test results (e.g. Nunez et el. 1987, McVay et al. 1998, Grundhoff et at. 1997, Dyson and Randolph 2001) are available in the literatures which were used in the previous studies for model verification.

The purpose of this paper is to present a series of three-dimensional finite element analysis of a long steel pipe pile in sand subjected to lateral load. The finite element results are compared with LPILE analysis, and also with the results of a full-scale test. The limitations of the *p-y* curve method are discussed based on lateral response of the pile.

2. FINITE ELEMENT MODELLING

The numerical analyses presented in this paper are carried out using the finite element software ABAQUS/Standard 6.10-EF-1. The finite element results are verified using the full-scale test results reported by Cox et al. (1974). The full-scale test site was located at the Shell Oil Company tank battery on Mustang Island, near Port Aransas, Texas. The test setup is shown in Figure 1.

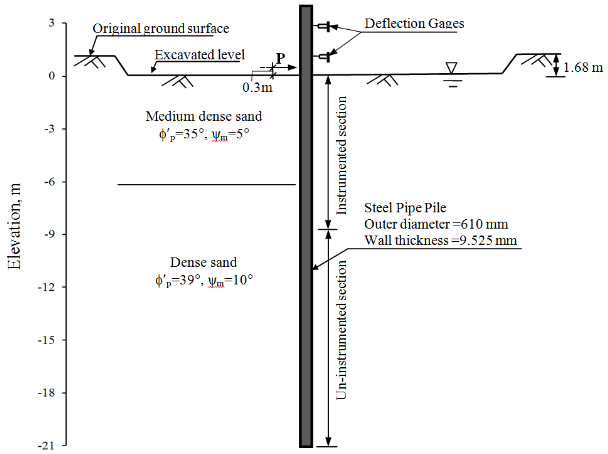

Figure 1 Idealized soil and pile load test setup (redrawn from Reese et al. 2001)

An excavation of 1.68m (5.5 ft) was carried out first to remove the soil near the ground surface and to reach the groundwater table. There was a clay layer of 0.76m (2.5 ft) near the groundwater table. This clay layer was also removed and filled with clean sand similar to in-situ condition. Pile load tests were conducted for static and cyclic loading. In this paper comparison is performed only with the test results of single pile under static load. Lateral load tests were conducted for a steel pipe pile of 610mm diameter and 9.53mm wall thickness. As shown in Figure 1, the top 9.75m length of the test pile was instrumented to obtain the response of pile under lateral load. A total of 40 strain gages were placed in the instrumented section of the pile. Lateral load was applied at 0.3m above the ground surface using a hydraulic jack and the load was measured using a universal load cell. The lateral deflection under a given lateral load was measured at two points above the load using two deflection gauges. The data was analyzed and response was reported for lateral load increments of 11.1kN up to 66.6kN and then in an increment of 5.56kN to the maximum lateral load of 266.9kN.

The finite element modeling in this study is carried out in Lagrangian framework. Considering geometry of the problem and loading conditions, the advantage of symmetry is used and only the half of the model under lateral load is analyzed. A soil domain of 20m diameter and 30m height as shown in Figure 2 is modeled. The pile is located at the center of the soil domain. The size of the soil domain is sufficiently large and therefore boundary effects are not expected on predicted lateral load, displacement and deformation mechanisms. The bottom of the soil domain is restrained from any vertical movement, while the curved vertical face is restrained from any lateral movement using roller supports. The symmetric vertical *xz* plane is restrained from any movement in the *y*-direction. No displacement boundary condition is applied on the top, and therefore the soil can move freely.

Both soil and pile are modeled using the solid homogeneous C3D8R elements, which are 8-noded linear brick element with reduced integration and hourglass control. The size of the mesh has a significant effect on finite element modeling. Often finer mesh yields more accurate results but computational time is higher. For successful FE modeling, finer mesh is used in the critical sections. The top five to ten pile diameters depth is critical for modeling piles under lateral load. Therefore, finer mesh is used for the upper 6.0m soil and medium mesh is used for 6.0 to 21.0m depth. For the soil layer below the pile (>21m depth) coarse mesh is used, as it does not have significant effect on load-displacement behaviour of the pile. Based on mesh sensitivity analyses with different mesh size and distribution, the optimum mesh consists of 18,027 C3D8R elements, shown in Figure 2 is selected for the present FE analysis.

3. MODELING OF PILE AND SOIL/PILE INTERFACE

A free-head steel pipe pile of 610mm (24″) outer diameter with 9.53mm (3/8″) wall thickness is modeled in this study. The embedded length of the pile is 21m. Lateral displacement is applied at 0.3m above the ground surface. Summing the nodal force component in the *x*-direction at at the point of loading, the lateral force is calculated. The pile is modeled as linear elastic material with modulus of elasticity (E_p) of 208×10^6 kN/m^2 and Poisson's ratio (ν_p) of 0.3. As shown later, the stress in the pile remains below the elastic limit even at the maximum displacement applied and therefore the modeling of the pile as elastic material is valid.

The Coulomb friction model is used for the frictional interface between the outer surfaces of the pile and sand. In this method, the friction coefficient (μ) is defined as $\mu=\tan(\phi_\mu)$, where ϕ_μ is the pile/soil interface friction angle. The value of ϕ_μ depends on surface roughness of the pile and effective angle of internal friction, ϕ'. Kulhawy (1991) recommended the value of ϕ_μ for steel pipe piles in the range of $0.5\phi'$ to $0.9\phi'$, where the lower values are for smooth steel piles. The value of μ=0.4 is used in this study.

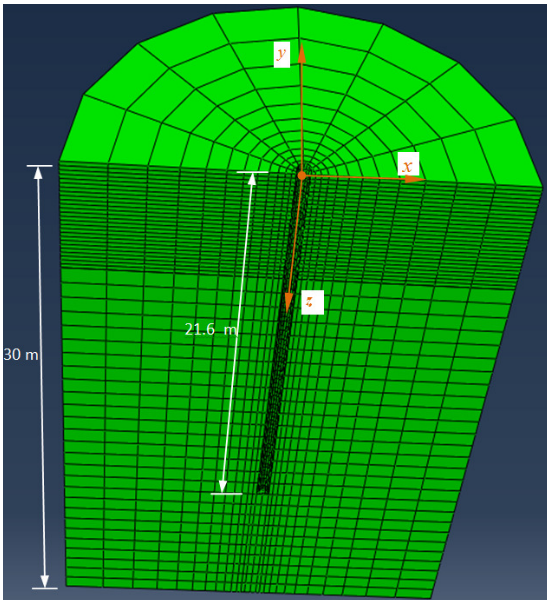

Figure 2 Finite element model

4. MODELING OF SOIL

Two boreholes were drilled at the Mustang Island pile load test site. Field tests and laboratory experiments on collected soil samples from these boreholes were conducted for geotechnical characterization (Cox et al. 1974). It was shown that the soil at the pile load test site is mainly sand with varying fine contents and relative density. Approximately 3m thick soft to stiff clay with shell fragments was encountered at 12.5m depth. As this clay layer has very small effect on lateral response it is ignored in the idealized soil condition used in the present study as shown in Figure 1. In the present study this clay layer is neglected as it does not have significant effect on lateral behaviour of the pile. The top 0–6m is a medium dense sand layer followed by a dense sand layer. Based on borehole logs, the soil profile is idealized as two sand layers for numerical analyses as shown in Figure 1. The geotechnical parameters used in numerical analyses are shown in Table 1. These parameters are estimated from the information provided in borehole logs and soil investigation.

Table 1 Geometry and mechanical properties used in finite element analysis

Pile:	
Length of the pile (L)	21.6 m
Diameter of the pile (D)	610 mm (24″)
Thickness of the pile (t)	9.53 mm (3/8″)
Modulus of elasticity of pile (E_p)	208×10^6 kN/m^2
Poisson's ratio (ν_p)	0.3
Soil (sand)	
Poisson's ratio, ν_s	0.3
Submerged unit weight of soil, γ'	10.4 kN/m^3
Upper medium sand (0 to 6m depth)	
Reference modulus of elasticity, E_{ref}	120,000 kN/m^2
Angle of internal friction, ϕ'_p	35°
Maximum dilation angle, ψ_m	5°
Initial modulus of subgrade reaction (k)	21,000 MPa/m
Lower dense sand (6 to 30m depth)	
Reference modulus of elasticity, E_{ref}	140,000 kN/m^2
Angle of internal friction, ϕ'_p	39°
Maximum dilation angle, ψ_m	9°
Initial modulus of subgrade reaction (k)	36,000 MPa/m

When a dense sand specimen is sheared in drained condition the shear stress increases with shear displacement as shown in Figure 3. The shear stress is reached to the peak at a relatively small strain and then strain softening is occurred. The strain at which the peak shear stress is developed depends upon mainly density of soil and applied normal/confining stress. At large displacement the shear stress remains constant which is considered as the critical state. The volume of a dense sand specimen is increased with shear displacement, which is normally characterized by dilation angle (ψ). At the critical state, shearing is occurred at constant volume. Most of the numerical analyses conducted in the past for modeling laterally loaded piles used a constant value of ϕ' and ψ. An appropriate value between the peak and ultimate condition is needed for this type of analyses.

In the present FE analysis the strain softening behavior is modeled by varying the mobilized friction angle (ϕ') and dilation angle (ψ) with plastic shear strain. The variation of ϕ' and ψ for medium and dense sand used in the analysis are shown in Fig. 3. The critical state friction angle (ϕ'_c) of 31° is used. Based on a large number of experimental data, Bolton (1986) showed that the angle of internal friction is related to the angle of dilation as $\phi' = \phi'_c + 0.8\psi$, which is used to calculate the mobilized dilation angle shown in Figure 3.

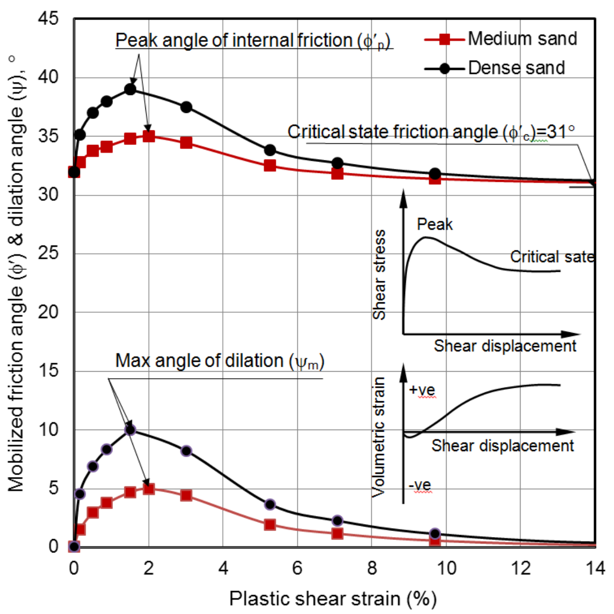

Figure 3 Mobilized angle of internal friction and dilation angle with plastic strain

The selection of appropriate values of elastic properties is equally important as the response of a pile depends on these parameters. In this study isotropic elastic properties are used. Experimental studies (e.g. Janbu, 1963; Hardin and Black, 1966) show that the elastic moduli of granular materials increase with the increase in mean effective stress (p'). It has been also shown by previous researchers that the elastic modulus depends on void ratio. Various expressions have been proposed in the past in order to account the effects of void ratio and mean effective stress on elastic moduli. Yimsiri (2001) compiled the available expressions in the literature. Based on these studies, the modulus of elasticity (E) is varied with mean effective stress (p') as

$$E = E_0\left(p'/p_a\right)^n \tag{1}$$

Where p_a is the atmospheric pressure (100 kPa) and n is a constant. The reference modulus of elasticity (E_0) represents the value of E at p'=100 kPa. Experimental results show that the value of n is approximately equal to 0.5 for sands (Yimsiri 2001).

The built-in Mohr-Coulomb model in ABAQUS/Standard is incapable of simulating the varying modulus of elasticity as a function of means effective stress and the post-peak strain softening behaviour of sand. Therefore, in this study they are incorporated in ABAQUS/Standard using a user subroutine called USDFLD written in FORTRAN. The mean effective stress and plastic shear strain is called at each time increment and two field variable is defined using these values. The model parameters E, ϕ' and ψ are updated based on these field variables.

The top layer of soil (0–6m) is medium dense sand which is modeled using the following soil parameters: angle of internal friction at the peak, ϕ_p'=35°; maximum dilation angle, ψ_m = 5°; reference modulus of elasticity, E_0 = 120,000 kPa; and Poisson's ratio, ν=0.3. The soil layer below 6m is dense sand. The soil properties used for this layer are: ϕ_p'=39°, ψ_m = 9°, E_0 = 140,000 kPa, and ν=0.3. The location of the groundwater table is at the ground surface. Submerged unit weight of 10.4 kN/m^3 is used for both soil layers.

5. LPILE ANALYSIS

Analysis of pile under lateral static load is also conducted using LPILE Plus 5.0 (2005) software. LPILE is a finite difference software where the pile is modeled as a beam with lateral stiffness based on elastic modulus and moment of inertia of the pile. The nonlinear *p-y* curves are defined using the method proposed by Reese et al. (1974). In this method the ultimate soil resistance per unit length of the pile is calculated using the angle of internal friction of the soil. The initial straight-line portion of the *p-y* curve is defined using the initial modulus of subgrade reaction (k). The variation of k with ϕ' and relative density is shown in Figure 4 as recommended by the American Petroleum Institute (API, 2000). The selection of an appropriate value of ϕ' is very important in LPILE analysis as the effect of dilation angle and post-peak softening of dense sand cannot not be directly used in this software. The angle of internal friction ϕ' in the horizontal axis at the top of Figure 4 is related to relative density as $\phi' = 16D_r^2 + 0.17D_r + 28.4$, where ϕ' is in degree, and D_r is the relative density (API 1987). Using the value of ϕ' calculated from this equation, Rollins et al. (2005) showed that it underestimates the friction angle and predicts significantly higher lateral displacement and bending moment compared to pile load test results. Therefore, in the present LPILE analyses ϕ'=35° for medium and ϕ'=39°for dense sand is used, which is consistent with Reese et al. (1974).

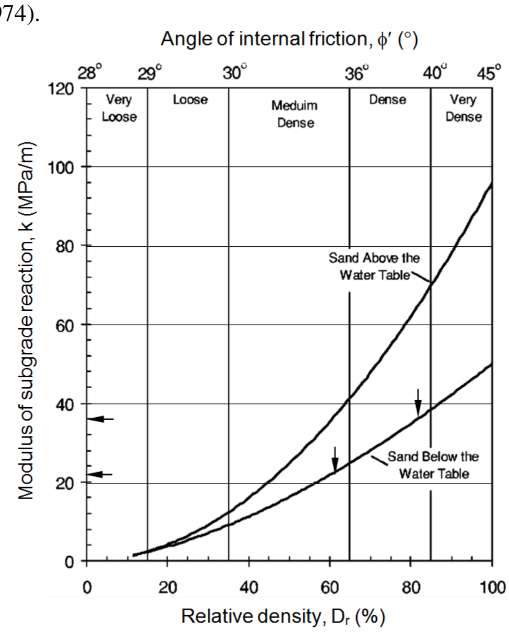

Figure 4 Lateral modulus of subgrade reaction as function of relative density and friction angle (API 2000)

6. NUMERICAL RESULTS

The finite element analysis consists of mainly two major steps: gravity step and loading step. In gravity step the soil domain is reached to the in-situ stress condition. In loading step the lateral displacement in the *x*-direction is applied on the nodes of the pile at 0.3 m above the ground surface.

6.1 Load-deflection curves

Figure 5 shows the variation of lateral load with lateral displacement of the pile at the ground surface obtained from finite element analysis and LPILE analysis. The results of full-scale test (Cox et al. 1974) are also shown in this figure.

In finite element analysis the lateral displacement is applied at 0.3m above the ground surface. The lateral load is calculated by adding the horizontal (*x*) component of nodal force at this level. The lateral displacement at the ground level is calculated by averaging the lateral displacement of all the nodes of the pile at ground level.

In LPILE the lateral load is applied in 11 increments. The pile is divided into 100 small divisions. The lateral displacement at the ground surface is obtained from the displacement of the element at this level.

Figure 5 shows a very good agreement between the full-scale test results and present finite element analysis. LPILE computed displacement for a given lateral load is higher than the measured displacement.

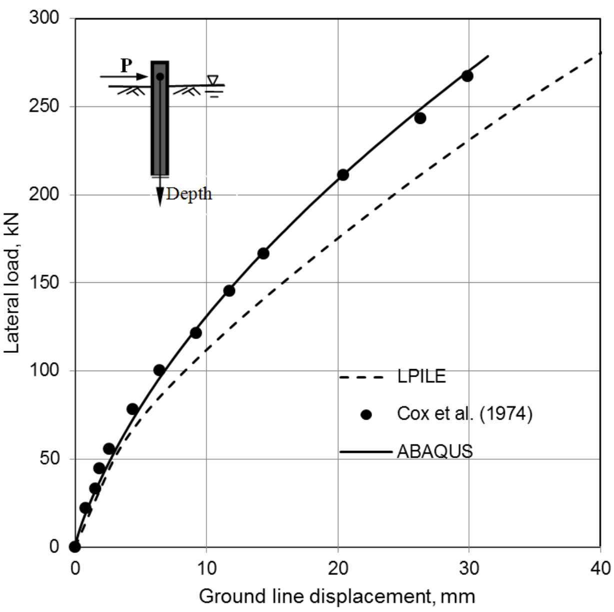

Figure 5 Comparison of load displacement between numerical predictions and full-scale test result

6.2 Bending moment with depth

Figures 6 (a-d) shows the variation of bending moment with depth for the upper 6m length of the pile. In these figures the depth in the vertical axis represents the distance from the point at which the lateral load is applied on the pile. Although the pile is 21m length the variation of bending moment only for upper 6m is shown because the maximum bending moment and its variation mainly occur in this zone. Comparison between computed and measured values for 11 lateral load cases (33.4kN, 55.6kN, 77.8kN, 101.1kN, 122.3kN, 144.6kN, 166.8kN, 189kN, 211.3kN, 244.6kN, and 266.9kN) are presented in these figures. In finite element analyses the bending moment is obtained from the axial stresses in the pile. In LPILE it can be easily obtained as the pile is modeled as a beam. The computed bending moment in the present finite element analysis compares very well with the measured data. However, LPILE compute higher bending moment than measured in the full-scale test.

The depth at which the maximum bending moment is occurred in the finite element analysis is less than that of LPILE analysis. For example, the maximum bending moment for 266.9kN is obtained at 2.5m if FE analysis while it is at 3.0m in LPILE analysis (Figure 6d).

It is to be noted here that the pile is in elastic condition even at the maximum lateral load applied. For the maximum lateral load of 266.9kN the computed maximum bending moment is 550kN-m. This gives the maximum tensile/compressive stress of 175MPa, which is less than yield strength of steel. That means, the analyses conducted in this study using elastic behaviour of the pile is valid even for the highest lateral load.

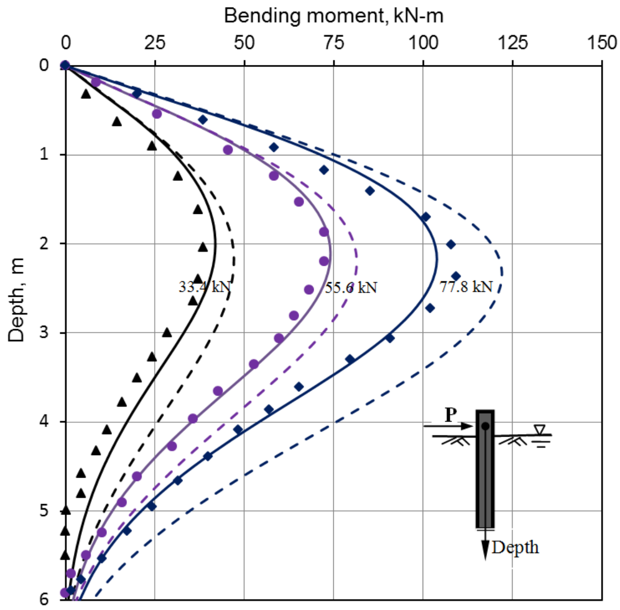

Figure 6(a) Variation of bending moment with depth (Load cases: 33.4kN, 55.6kN and 77.8kN; solid lines: FE analysis, dashed line: LPILE and data points: full-scale test)

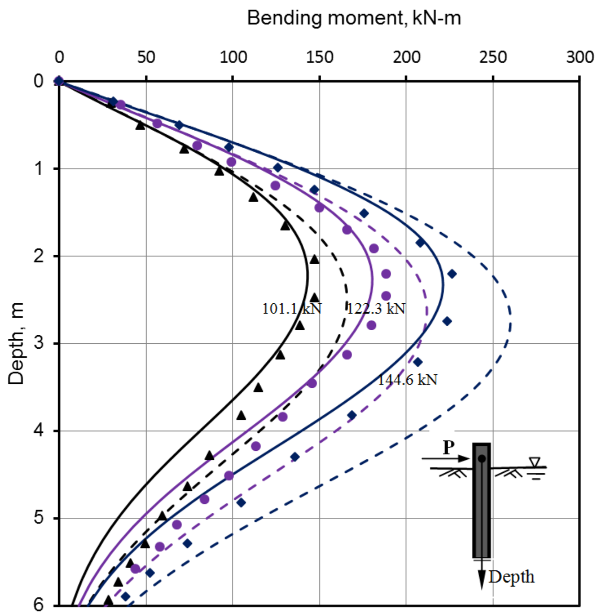

Figure 6(b) Variation of bending moment with depth (Load cases: 101.1kN, 122.3kN and 144.6kN; solid lines: FE analysis, dashed line: LPILE and data points: full-scale test)

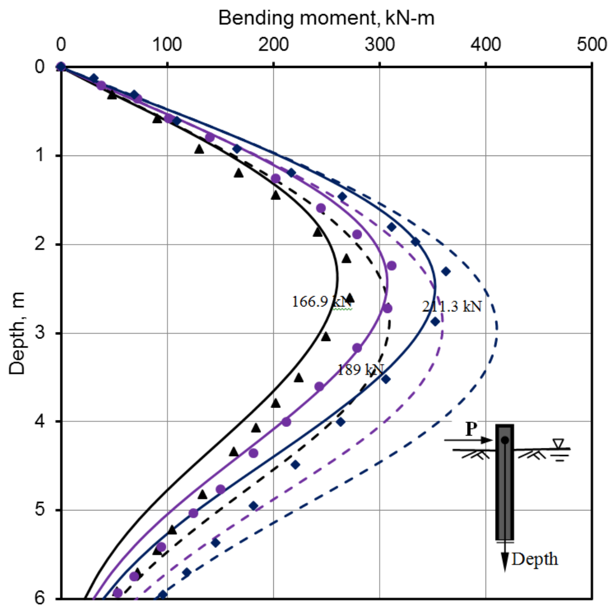

Figure 6(c) Variation of bending moment with depth (Load cases: 166.8kN, 189kN and 211.3kN; solid lines: FE analysis, dashed line: LPILE and data points: full-scale test)

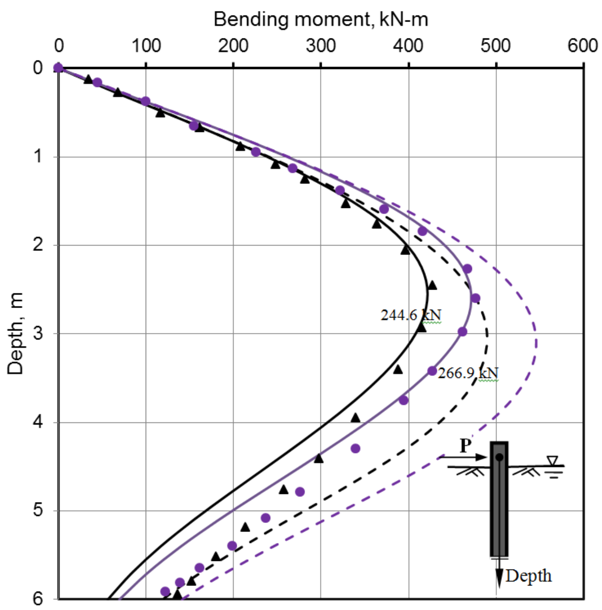

Figure 6(d) Variation of bending moment with depth (Load cases: 244.6kN and 266.9kN; solid lines: FE analysis, dashed line: LPILE and data points: full-scale test)

6.3 Maximum bending moment

Figure 7 shows the variation of the maximum bending moment with lateral load. The maximum bending moment increases with increase in lateral load. At low values of lateral load, both finite element and LPILE compare well with full-scale test data. However, at larger loads the computed maximum bending moment using LPILE is higher than the values obtained from the present finite element analysis and full-scale test.

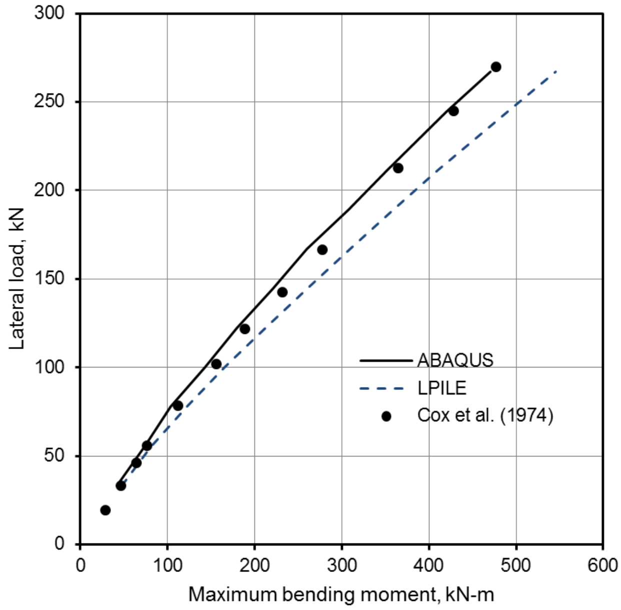

Figure 7 Comparison of maximum bending moment and lateral load

6.4 Lateral displacement

Figure 8 shows the computed lateral displacement of the pile with depth for 11 load cases for FE and LPILE analyses. As shown in this figure that LPILE predicts higher lateral displacement than the present FE simulation. For comparison with field data the displacement at the ground surface obtained in the full-scale test is also shown in this figure by solid circles, which match very well with the present FE analysis.

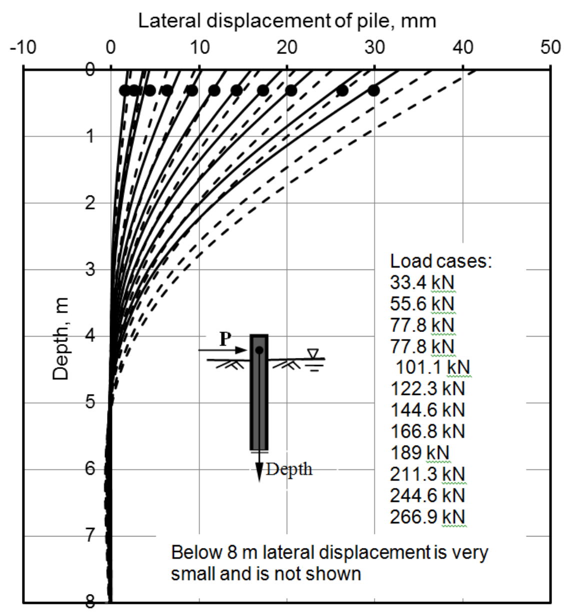

Figure 8 Lateral displacement of pile (solid lines: FE analysis; dashed line: LPILE: solid circles: measured at ground line in pile load test)

6.5 Soil reaction

Lateral soil reaction (force per metre length of the pile) is plotted in Figure 9. For clarity the calculated results for 5 load cases are shown in this figure. In finite element analysis, the x-component (lateral) of nodal force is calculated first for all the nodes at a given depth. Dividing the sum of the nodal force in the x-direction by the vertical distance between two sets of nodes in the pile, the lateral soil reaction is obtained. In LPILE analysis the soil reaction can be easily obtained from the output file as the pile is modeled as a beam supported by discrete springs. As shown in this figure that calculated soil reaction from both LPILE and FE is very similar up to 1.2m depth. However, below 1.2m the soil reaction obtained from the FE analysis is higher than the reaction obtained from LPILE. Moreover, after reaching to the maximum value of soil reaction, it decreases quickly with depth in the finite element analysis. The maximum soil pressure is developed at greater depth for larger value of lateral load.

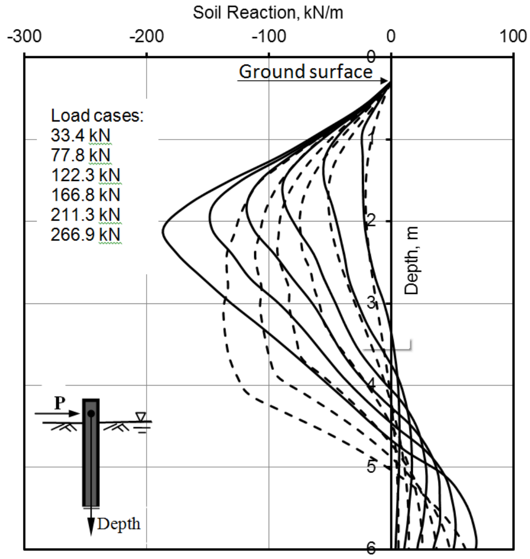

Figure 9 Soil reaction on pile (solid lines: FE analysis and dashed line: LPILE)

6.6 Shear force in pile

Figure 10 shows the variation of shear force in the pile with depth for five lateral loads. In the finite element analysis the shear force is obtained by subtracting the sum of the *x*-component of nodal force above the point of interest from the lateral load applied at pile head. As shown in Figure 9 that the calculated soil reaction in the finite element analysis is higher near the ground surface. Therefore, the shear force is decreased quickly in the finite element analysis near the ground surface as shown in Figure 10. The maximum negative shear force from LPILE analysis is higher than that obtained from the finite element analysis. Below the depth of 9m the shear force is negligible.

6.7 *p-y* curves

In the current engineering practice the modeling of a laterally loaded pile is generally performed as a beam on elastic foundation, where soil is modeled by discrete springs. The load deformation behaviour of the soil spring is defined using nonlinear *p-y* curves. The *p-y* curves for four depths are shown in Figure 11. In LIPILE the *p-y* curve for a given depth can be easily obtained from the output file. In the finite element analysis the soil is modeled as a continuum, not as discrete springs. The values of *p* and lateral displacement are calculated from nodal forces and displacement, respectively. In this study the model proposed by Reese et al. (1974) for static lateral loading is used in LPILE analysis. The *p-y* curve in Reese et al. (1974) consists of four segments (Figure 11): (i) initial linear segment, which is mainly govern by *k* value, (ii) parabolic segment between the initial linear segment and lateral displacement of D/60, (iii) linear segment between lateral displacements of D/60 and 3D/80, and (iv) constant soil resistance segment after lateral displacement of 3D/80. The *p-y* curves obtained from the finite element and LPILE analyses are also compared with full-scale test data (Cox et al. 1974). As shown in Figure 11, the *p-y* curves obtained from the finite element analysis match better with the measured values.

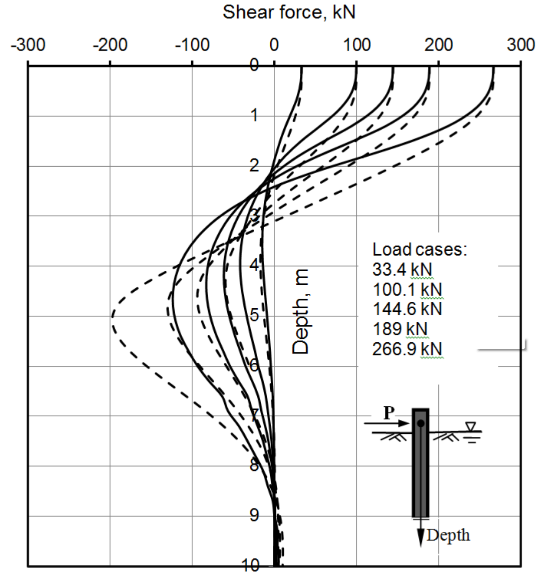

Figure 10 Variation of shear force in pile with depth (solid lines: FE analysis, dashed line: LPILE)

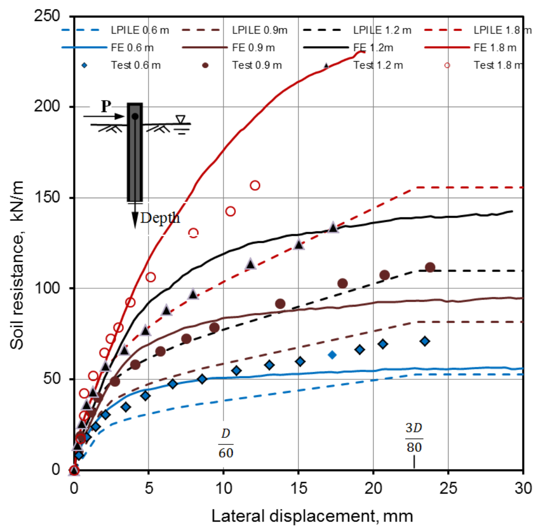

Figure 11 Comparison of p-y curves at four depths (solid lines: FE analysis, dashed line: LPILE, and data points: full-scale test)

7. DISCUSSION AND CONCLUSIONS

The *p-y* curve based software packages, such as LPILE, are widely used in engineering practice to calculate the load-displacement behavior of laterally loaded piles. Although this method is very simple, it has a number of limitations. The soil resistance is modeled as discontinuous nonlinear springs defining the properties empirically. Moreover, the pile/soil interface behavior cannot be modeled in the *p-y* curve method. In the present study three-dimensional finite element analyses are performed for a laterally loaded flexible pile in sand. Analyses are performed using a modified form of Mohr-Coulomb soil constitutive model, where the variation of mobilized angle of internal friction and dilation angle with plastic shear strain is considered. The non-linear variation of elastic modulus with mean effective stress is also considered in the present FE analyses. Numerical analyses are also performed by using the commercially available LPILE software. The geotechnical parameters require in the FE analysis can be easily obtained from the conventional laboratory shear strength tests. The variation of mobilized friction angle and dilation angle with plastic shear strain can be obtained from triaxial test data. On the other hand, the post-peak softening behavior cannot be incorporated in the *p-y* curve method. Therefore, a constant representative value of ϕ' between the peak and critical state is required to be selected. The initial modulus of subgrade reaction (k) is also related to ϕ' and relative density as shown in Figure 4. Note that k is not a fundamental soil property. Consider a pile foundation in dense sand having the peak and critical state friction angles of 41° and 31°. For successful prediction of the response of a laterally loaded pile using the *p-y* curve method a representative value of ϕ' between 41° and 31° is needed. API (1987) recommended an empirical equation for estimating the representative value of ϕ' as a function of relative density. However, the computation with this recommended value of ϕ' over predicts the maximum bending moment and lateral displacement (Rollins et al. 2005). The limitations of the *p-y* curve method could be overcome by using FE modeling as presented in this paper. The response of the pile is calculated using the fundamental soil properties such as friction angle, dilatancy and stiffness. It is also shown that the FE model can successfully simulate the full-scale test results.

8. REFERENCES

American Petroleum Institute (API). (1987). "Recommended practice for planning, designing and constructing fixed offshore platforms", API Recommended practice 2A (RP 2A), 17th Ed.

American Petroleum Institute (API). (1993) Recommended Practice for Planning, Designing and Constructing Fixed Offshore Platforms – Working Stress Design, API Recommended Practice 2AWSD (RP 2A-WSD), 20th edition, p191

API (2000). "Recommended practice for planning, designing and constructing fixed offshore platforms working stress design", RP2A-WSD 21st ed., American Petroleum Inst.

Ashour, M., and Norris, G., (2000). "Modelling lateral soil- pile response based on soil-pile interaction, J. of Geotechnical and Geoenvironmental Engineering", 126(5), pp. 420-428.

Bolton, M., The strength and dilatancy of sands. Geotechnique 1986;36(1), pp. 65–78.

Broms, B., (1964a). "The Lateral resistance of piles in cohesive Soils", J. Soil Mech. Found. Div., ASCE, 90, pp. 27-63.

Broms, B., (1964b). "The lateral resistance of piles in cohesive soils", J. Soil Mech. Found. Div., ASCE, 90, pp. 123-156.

Brown, D. A., (1985). "Behaviour of a large scale pile group subjected to cyclic lateral loading, Ph. D. Thesis", University of Texas at Austin.

Brown DA, Shie C-F. (1991). "Some numerical experiments with a three dimensional finite element model of a laterally loaded pile", Computers and Geotechnics, 12, pp. 149–162.

Cox, W. R., Reese, L. C., and Grubbs, B. R., (1974). "Field testing of laterally loaded piles in sand", Proc. 6th Annual Offshore Technology Conf., Houston, OTC2079.

Dyson, G.J., Herdsman, Randolph, M.F., (2001). "Monotonic lateral loading of piles in calcareous sand", Journal of Geotechnical and Geoenvironmental Engineering, v 127, n 4, pp. 346-352.

Earth, J. B., and Geo, W. P., (1991) "Asian geotechnical amongst authors of conference Publications", Proceedings of Int. Conference on Asian Geotechnical, Hong Kong, pp133-137.

Finn, W. D. L., and Fujita, N. (2002) "Piles in liquefiable soils: seismic analysis and design issues". Soil Dynamics and Earthquake Engineering, 22, Issues 9-12, pp731-742.

Grundhoff, T., (1997). "Horizontal impact loads on large bored single piles in sand", Proceedings of the International Offshore and Polar Engineering Conference, v 1, pp. 753-760, 1997

Hansen, Brinch J. (1961). "The ultimate resistance of rigid piles against transversal forces", Danish Geotechnical Institute (Geoteknisk Institut) Bull. Copenhagen, 12:5-9.

Hardin, B.O. and Black, W.L. (1966). "Sand stiffness under various triaxial stresses", Journal of the Soil Mechanics and Foundations Division, ASCE, Vol. 92, No. SM2, pp. 27-42.

Janbu, N. (1963). "Soil compressibility as determined by oedometer and triaxial tests", Proc. Euro. Conf Oil Soil Mech. 111/1.1 FUUlld. Ic·llgrg., German Society for Soil Mechanics and Foundation Enginec:ring, Wissbaden, Germany, Vol I, 1925.

Kimura M, Adachi T, Kamei H, Zhang F. (1995). "3-D finite element analyses of the ultimate behaviour of laterally loaded cast-in-place concrete piles", In Proceedings of the Fifth International Symposium on Numerical Models in Geomechanics, NUMOG V, pp. 589–594.

Kulhawy, F. H. (1991). "Drilled shaft foundations, Chapter 14 in Foundation Engineering Handbook", 2nd ed, Hsai-Yang Fang Ed., Van Nostrand Reinhold, New York.

LPILE Plus 5.0 (2005). ENSOFT, INC., 3003 West, Howard Lane, Austin, Texas 78728.

Long, J. H., and Reese, L. C., (1985). "Methods for predicting the behaviour of piles subjected to repetitive lateral loads", Proc., 2nd Shanghai Symp. On Marine Geotechnology and Nearshorea Offshore Structures, Shanghai, Chaina.

Meyerhof, G. G., Sastry, V. V. R. N. and Yalcin, A. S. (1988). "Lateral resistance and deflection of flexible piles", Canadian Geotechnical Journal, 25(3), pp. 511-522.

Meyerhof. G, G., Mathurs, S. K., and Valsangkara, A. J. (1981). "Lateral resistance and deflection of rigid walls and piles in layered soils", Canadian Geotechnical Journal, 18, pp. 159-170.

McVay, M., Zhang, L., Molnit, T., and Lai, P. (1998). "Centrifuge testing of large laterally loaded pile groups in sands", J. Geotech. Geoenviron. Eng., 124(10), pp. 1016–1026.

Nunez, I.L., Phillips, R., Randolph, M.F., and Wesselink, B.D. (1987). "Modelling laterally loaded piles in calcareous sand", Cambridge University, Engineering Department, (Technical Report) CUED/D-Soils.

Poulos, H.G., (1971). "Behaviour of laterally loaded piles", I- Single piles, J. of the Soil Mechanics and Foundations, Div. 97(5), pp. 711-731.

Reese, L. C., Cox, W. R., and Koop, F. D. (1974). "Analysis of laterally loaded piles in sand", Proc. 5th Annual Offshore Technology Conf., Houston, OTC2080.

Reese, J. C. & Van Impe, W. F., (2001). "Single piles and pile groups under lateral loadings", A. A. Balkema, Rotterdam.

Rollins, K. M., Lane, J. D., and Gerber, T. M., (2005). "Measured and computed lateral response of a pile group in sand", J. Geotech. Geoenviron. Eng., 131(1), pp. 103-114.

Ruesta, P. F., and Townsend, F. C. (1997). "Evaluation of laterally loaded pile group at Roosevelt Bridge", J. Geotech. Geoenviron. Eng., 123(12), pp. 1153–1161.

Trochanis AM, Bielak J, Christiano P. (1991). "Three-dimensional nonlinear study of piles. Journal of Geotechnical Engineering", 117(3), pp. 429–447.

Wakai A, Gose S, Ugai K. (1999). "3-d Elasto-plastic finite element analysis of pile foundations subjected to lateral loading", Soil and Foundations, 39(1), pp. 97–111.

Yang, Z., and Jeremic, B., (2002). "Numerical analysis of pile behavior under lateral loads in layered elastic-plastic soils", Int. J. for Numerical and Analytical Mehods in Geomechanics, 26, pp. 385-1406.

Yimsiri, S. (2001). "Pre-failure deformation characteristics of soils: anisotropy and soil fabric", Ph.D. Dissertation, University of Cambridge, Cambridge, England.